Efficient and Accurate Phase Unwrapping Algorithms for Noisy Images within Fringe Patterns

Samia HESHMAT
Candidate for the Degree of Doctor of Philosophy
Supervisor: Assoc. Prof. Satoshi TOMIOKA
Division of Quantum Science Engineering

Introduction

Phase unwrapping is a crucial and challenging step to most data-processing chains based on phase information in many fields of research, such as magnetic resonance imaging, synthetic aperture radar interferometry and optical metrology. In all these research fields, the measured parameters are modulated in the form of two-dimensional fringe pattern. To retrieve the phase information from the fringe pattern, Fourier domain filtering or phase shift technique can be used. The retrieved phase values, which are wrapped phase, are the distribution of principal values ranging from $-\pi$ to π. Thus, phase unwrapping procedure is needed to get back the unknown multiple of 2π to each pixel. This is why many algorithms have been proposed for phase unwrapping. However, there is no agreement between the current phase unwrapping algorithms for different applications, due to the existence of disturbance in the measured phase data. In the case that there is no disturbance in the phase data, the unwrapped phase can be obtained by integrating the phase gradients over the whole data samples, which is independent from the integration path. However, there are several sources of errors in the phase images. Firstly, phase aliasing occurs when the true phase changes by more than one cycle (2π rad) between samples, which was caused by long baselines, objects discontinuities or high deformation. The second source is noise, which may be caused by speckle noise, electronic noise and/or fringe breaks. Those defected points in the measured phase images are called singular points (SPs). To exclude these invalid areas from unwrapping process and get precise unwrapped phase results can be a time-consuming process.

For this purpose, we proposed a novel phase unwrapping algorithm for noisy phase images. The proposed algorithm is called rotational and direct compensators for phase unwrapping (RC+DC) **[1]**. The RC+DC algorithm is a new phase unwrapping approach for noisy wrapped phase maps of continuous objects to improve the accuracy and computational time requirements of phase unwrapping using a rotational compensator (RC) method.

Fringe analysis techniques are considered to be effective and reliable optical noncontact methods for surface shape measurements. In these techniques, a structured lighting pattern is projected onto the surface of an object. According to the surface shape of the object, the projected pattern will be modified. This pattern is captured by a CCD camera and then stored into computer memory. The image is then analyzed by one of fringe analysis algorithms to extract the phase information and retrieved the continuous form of the phase distribution by applied one of phase unwrapping methods. Finally, by using phase-height relationship, the object height shape can be determined. **Figure 1** is summarized these steps about fringe patterns analysis.

Driven by these motivations, both theoretical aspects of the phase unwrapping problem as well as practical algorithms for its solution is examined in this dissertation. However, we begin with a brief explanation for the main stages of fringe analysis methods to figure out the problems of phase processing and the circumstances in which they arise.

Phase extraction

Many techniques have been proposed for the analysis of fringe patterns. These techniques vary in accuracy, the number of frames required and processing time. The aim of any fringe pattern analysis algorithm is to obtain the phase information modulated into the fringe pattern. This phase is wrapped between $[-\pi, \pi)$ and needs to be unwrapped. Fringe pattern analysis algorithms can be classified into two categories, which are spatial and temporal techniques. Spatial methods calculate the phase of a pixel in a fringe pattern depending on its neighboring pixels. Examples for spatial technique such as Fourier fringe analysis and direct phase demodulation. Spatial

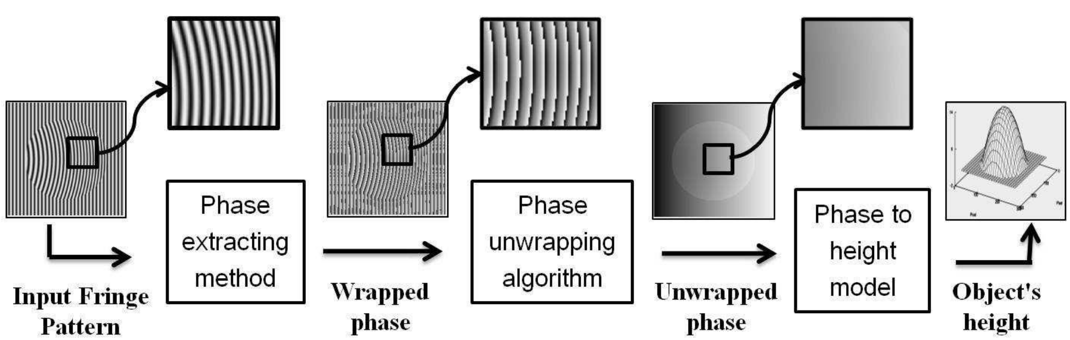

***Figure 1**: Fringe analysis for an object*

techniques require at least one fringe pattern to calculate the phase components. In contrast, temporal algorithms require at least three images to calculate the phase of a pixel depending on the values of that pixel in different images and independent of its surrounding pixels. An examples of a temporal methods is phase stepping. However, in this study our main concerning is for the unwrapping stage in the analysis of fringe pattern process.

Phase unwrapping

Phase unwrapping is a technique used on wrapped phase images to remove the 2π discontinuities embedded within the phase map. It detects a 2π phase jump and adds or subtracts an integer offset of 2π to successive pixels following a threshold mechanism, thus, retrieving the contiguous form of the phase map.

Commonly, most of phase unwrapping algorithms are based on one assumption that the true unwrapped phase data varies slowly enough that neighboring phase differences values are within one half cycle (π radian) of each other. If this assumption is true everywhere the unwrapping process can be applied simply by integrating wrapped phase differences, or gradients, along any path from pixel to pixel throughout the phase data to obtain unwrapped phase. In one-dimensional phase unwrapping, this process is repeated from first end point region (first pixel) toward the second end point region (last pixel); hence, the phase difference can be calculated as follows:

$$\triangle\Psi^{i} = \Psi_{i} - \Psi_{i-1} \tag{1}$$

where Ψ^{i} is the wrapped phase at pixel i in phase map. When the phase difference, $\triangle\Psi^{i}$ is larger than a half cycle the wrapped phase is shifted one cycle, so the shifted difference is again smaller than a half cycle. This shift operation is same as the wrapping operation used to obtain the principal value of the true phase. The wrapping operator is defined as follows:

$$\Psi_{i} = W[\Phi_{i}] \cong \Phi_{i} - \mathrm{Int}\left[\frac{\Phi_{i}}{2\pi}\right] 2\pi \tag{2}$$

where $-\pi < W[\Phi_i] \leq +\pi$, Φ_i is the continuous true phase at pixel i in phase map and Int[.] means a function that returns the nearest integer. The wrapping operator W[.] could be modified to specify the corrected gradient phase difference between two successive pixels in the unwrapping path as:

$$\hat{\nabla}\Psi^{i} = W[\Psi_{i} - \Psi_{i-1}] \tag{3}$$

In two-dimensional phase unwrapping, there are paths with loop; it means that the last point can be considered as the first point. In the absence of discontinuity sources, the unwrapped result is independent on the unwrapping path; therefore, the unwrapped phase map is consistent. Consider that the path of loop consists of M points, using Eqs. (1)-(3) we can retrieve the true unwrapped phase as follows:

$$\Phi_{M} = \Phi_{0} + \sum_{i=1}^{M} \hat{\nabla}\Psi^{i} \tag{4}$$

To find SPs, which are the error sources in the phase unwrapping process; consider a closed path starting in every point defined by the corners of a 2 × 2 square along the closed path in clockwise direction The SPs are marked the start and end of 2π discontinuity line. They are identified by summing the wrapped phase gradient, as follows:

$$\sum_{i=1}^{N} \hat{\nabla}\Psi^{i} = 2\pi S \tag{5}$$

where S is the SP residue. The SP is called a positive residue when S in Eq. (5) is +1; otherwise, it is called a negative residue when S is −1. While, S = 0 indicates that no residue exists.

In order to solve inconsistencies caused by SPs, many phase unwrapping algorithms have been proposed in the past, they can be divided into two categories. The first category contains algorithms based on following the paths [3–8]. These methods involve integrating the phase gradient of pixels in an image over a path starting from a certain point and going over all the pixels, in essence, unwrapping the image. Path independent unwrapping is obtained in the absence of error sources (singular points) that can arise from either noise or object discontinuities. The unwrapped result is independent of the unwrapping path; hence, the complete phase map is consistent. However, in the presence of corrupted pixels (singular points), taking just any path is not possible anymore. Consequently, unwrapping becomes path dependent, where it has to manoeuvre between pixels choosing the best path to follow where the pixels are not corrupted by error. To overcome path dependence, many ways have been suggested and implemented. Hence, it can be said that path following methods fist search for SPs, then pair these SPs by placing branch cuts. By examining the branch cuts and determining if any appear to be placed poorly or any isolate a region, it can be determined whether or not the paths can be followed to retrieve the phase maps, as well as whether these methods succeed or fail.

The second category includes the methods which use the least-squares approach [9–12]. These algorithms use a different way for unwrapping images while still using the estimated phase gradient. They use the same idea of minimization of discrete gradients difference squares as used in the leased-squares approach. These differences are taken between the wrapped phase gradients and supposed unwrapped phase gradients. In these methods, a smooth solution is achieved by the resultant minimization. That can be done by integrating over all the possible paths within the image not like path following methods, which integrate over one single path, thus, spreading the error over the whole image. Like the previous methods, these methods also encounter a large number of errors once a corrupted region is present in the image. Hence, weighting parameters are introduced to exclude corrupted regions. However, the success of algorithms using such a method relies on choosing the weights, which puts a huge load on the performance of the algorithm. One advantage of these methods over algorithms based on following the paths is unwrapping SPs rich regions.

Based on the above discussion, the existing phase unwrapping methods suffer from various problems that can affect time, cost, and accuracy of unwrapped results. Therefore, it is needed to investigate and improve the existing unwrapping methods. In this study, we attempt to reduce the computational time requirements of the RC method to a minimum, and to improve the level of efficiency and reliability as well. It was found that the distribution of dipole distance shows that there are a lot of dipole pairs that have short distances. According to this finding, the proposed algorithm is computing compensators for adjoining pairs of SPs directly; the new method is a coupling of the RC and the direct compensator (DC).

Phase Unwrapping algorithm based on RC and DC techniques

In a manner similar to the phase unwrapping algorithm developed by Tomioka et al. [2], the main issues determine the behavior of the proposed algorithm: the RC, unconstrained singular point positioning, and virtual singular points approaches to compensate the inconsistencies and to confine the effect of each one in a local region. The proposed algorithm is based on their method; however, the way of computing the compensators for adjoining SP pairs is different from RC. The following subsection explains and discusses the RC and DC principles and the description of the proposed algorithm.

Rotational compensator technique

Since phase unwrapping is an essential process of removing discontinuities by local neighborhood tests and corrections, the idea of compensator is proposed to compensate and cancel the singularity effect by the spreading singularity phase unwrapping (SSPU) [13] or RC methods [2]. The SSPU method requires iteration process to compute the compensators, while the RC method can compute the compensator by superposing the effect of each SP. RC can cancel singularity of each SP by adding an integral of isotropic singular function along any loops. When a closed loop includes SP, the integral along the loop will have a value of $-2\pi S$, where S is the residue of the SP shown in Eq. (5). Representing an integral of a segment i, which is a member of the loop comprising N segments, as C^i, we can reduce Eq. (5) as follows:

$$\sum_{i=0}^{N-1}(\hat{\nabla}\Psi^i + C^i) = 0. \qquad (6)$$

This suggests that the singularity of Ψ^i is regularized by compensator C^i, and phase unwrapping becomes an independent path. The RC for the i^{th} segment, which is a path from r_i to r_{i+1} to cancel the singularity of the j^{th} SP, ${}^{R}C^i_j$, is represented as follows:

$${}^{R}C^i_j = -S_j(\theta_{i+1,j} - \theta_{i,j}) \qquad (7)$$

where S_j denotes the residue of the j^{th} SP, and $\theta_{i+1,j}$ and $\theta_{i,j}$ are azimuthal angles of both ends of the i^{th} segment, where the origin is located at the j^{th} SP.

When the measured data contains several SPs, the total compensator of the ith segment is estimated as the summation of the ${}^{R}C^i_j$ with respect to j:

$${}^{R}C^i = \sum_{j=1}^{N_s} {}^{R}C^i_j \qquad (8)$$

Consequently, we can retrieve the true unwrapped phase data by summing the phase differences between the adjoining pixels and the total compensators as follows:

$$\Phi_M = \Phi_0 + \sum_{i=1}^{M}(\hat{\nabla}\Psi^i + C^i) \qquad (9)$$

where $C^i = {}^{R}C^i_j$.

It is noteworthy that Eq. (9) is the modification of Eq. (4) after removing the effect of SPs by compensating each SP with the compensator, which has the opposite sign of SP. However, if the measured phase data contains several SPs, the computation of each compensator becomes a time-consuming process. This is one of the drawbacks of the RC method. Another drawback is that the RC introduces an undesirable distortion of phase in a large area which is far from the areas with SPs. Since the RC for the i^{th} segment caused by the j^{th} SP, ${}^{R}C^i_j$, decreases with increasing the distance between the segment and the SP, the RC becomes small for the far segment. However, it is not exactly zero. This means that the RC affects the regular region and its effect is considered as an error of phase unwrapping.

Direct compensator technique

Every SP has a residue of ±1. A pair of two SPs with different polarity is considered as a dipole. It was found that the distribution of SP dipole distances shows that there are a lot of dipole pairs with short distances. We propose a new phase unwrapping algorithm based on this finding. The proposed algorithm reduces the drawbacks of the RC method, which are the high computational time cost and the undesired phase error due to its effect on the regular region. The proposed method compensates the singularities of adjoining SP pairs by adding the DC. Thus, the effect of each SP is confined in a closer local region. The RC computed by Eqs. (7) and (8) compensates the singularities of all SPs. The integral of the total RC along any closed path equals the negative sum of the residues of SPs in the domain surrounded by the closed path. In the case of DC, the domain is limited to a small region; however, the DC must have the same property. If the distance between two SPs with opposite polarity is one pixel, the DC is applied. The sum of the DC along the smallest path surrounding one of the two SPs, which consists of four segments, equals one cycle (2π radian). Furthermore, the sum of the DC along the path surrounding both SPs must vanish. A solution satisfying these conditions is obtained by setting of branch-cut. The branch-cut is placed between the two SPs. When the segment to unwrap crosses the branch-cut, the sum of DC for the two SPs is defined as one cycle. No DC is applied for the other segment.

The adjoining pair is a dipole, which consists of two SPs with the opposite polarities, separated by one pixel horizontally or vertically. **Figure 2** shows the configuration of the branch-cuts placed between the adjoining SPs in the phase map and the concept of the direct compensation. **Figure 2(a)** shows a case in which the branch-cut is placed between a pair

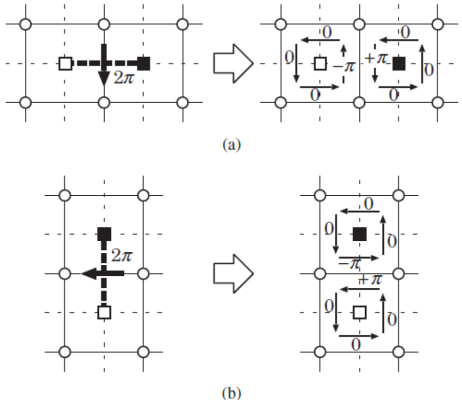

Figure 2*: Existence of the branch-cuts between adjoining SP pairs and the concept of direct compensation (DC). Open and filled squares represent positive and negative SPs, respectively. The thick dashed line denotes the branch-cut that connects two opposite sign SPs. Compensator positions are indicated by thick arrows. The thin arrows show the direction and distribution of compensators for the segments of each SP.*

of adjoining SPs horizontally, so that the DC will be added to the vertical segment that crosses the branch-cut. In contrast, **Fig. 2(b)** shows the case in which the branch-cut is placed vertically between the adjoining SPs and the DC is added horizontally. The compensator value of the segment is divided into two compensator values, and distributed through the two adjacent loops, which contain adjoining SP pairs, as illustrated in **Fig. 2**. The direction of the DC, ${}^{D}C^{i}_{j}$, for the segment is based on the position of this segment with respect to the location of the tested SP. Hence, the confinement of the DC effect in a closer region around the SPs leads to the improvement in the accuracy of the unwrapped phase results. When the segments are far from SPs, their DCs have zero value so that the computation of DC is not needed. In contrast, the RC requires computation according to Eq. (8). For this reason, the computation time requirements of the proposed algorithm for computing total compensators will be reduced and the accuracy of the unwrapped phase will be improved.

Description of proposed algorithm

The proposed method is based on coupling the RC and DC to compute the compensators in connection with the distance of SP pairs. In other words, it uses the DC for computing the compensators of adjoining SP pairs, and uses the RC to compute the compensators for other SP pairs. Therefore, the main steps in the proposed algorithm are as follows:

- If a pair of SPs is an adjoining pair, a DC will be added. Its value is π and the sign is dependent on the position of the segment with respect to the location of the tested SPs.
- In contrast, if a pair of SPs is not an adjoining pair, RC will be computed using Eq. (8).
- Finally, after computing the total compensators for each segment, the true unwrapped phase values can be retrieved by summing the phase differences between the adjoining pixels and the total compensators, as illustrated in Eq. (9).

This description of the direct compensation for adjoining SP pairs ensures that the proposed algorithm is simple and easy to implement. It provides a fast and efficient way to unwrap the phase map. The performance and applicability of the proposed algorithm are examined in the following section.

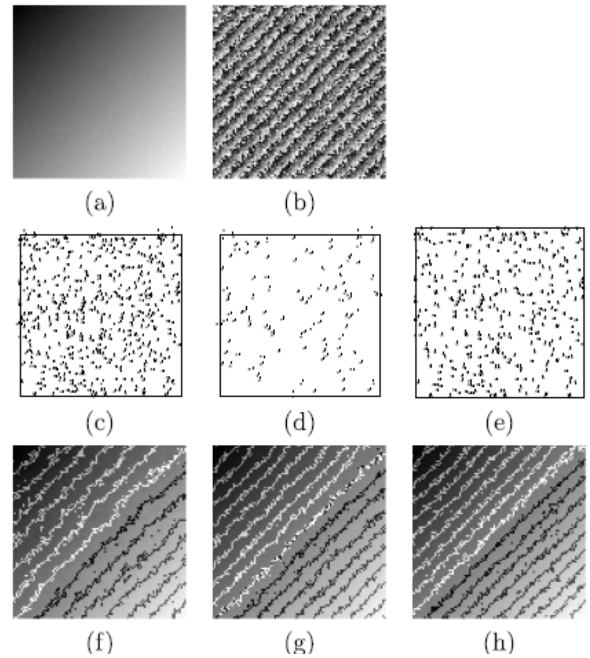

Figure 3*: A comparison of the unwrapped phase results for simulated phase data has noise with σ = 0.15 cycle: (a) the original phase data, (b) the wrapped data, (c) the positions of all SP pairs, (d) the positions of the pairs of non-adjoining SPs, (e) the positions of the pairs of adjoining SPs, (f) unwrapped result by LS-DCT, (g) unwrapped result by RC, and (h) unwrapped result by RC+DC. In (a), (b), and (f)-(h), the phase increases with the increases of brightness. In (f)-(h), contour lines of the phase with the interval of one cycle are also shown*

Results and discussion

To evaluate the performance of the proposed phase unwrapping algorithm, both simulated and real wrapped phase maps have been used. These phase data are the same data that were used in the study of RC [2].

Computer Simulation Results

In order to demonstrate the applicability of the proposed approach, a simulated noisy phase map with constant gradient is generated. This phase data has the image size 100 × 100 pixels^2, the gradient is (0.1, − 0.1) cycle/pixel, and the noise has a normal distribution with 0.15 cycle standard deviation. The original and wrapped phase data are shown in **Figs. 3(a)** and **3(b)**, respectively. In addition, **Fig. 3** presents the distribution patterns of SP pairs for real and virtual SPs to show the position of SP pairs in the phase map. In **Fig. 3(c)**, all SP pair positions are presented, while in **Figs. 3(d)** and **3(e)**, the positions of the pairs of non-adjoining and adjoining SPs are shown, respectively. This indicates that most of SP pairs in the phase map are adjoining pairs; therefore, the use

Table 1. *Comparison of the Accuracy for the Simulation Data Shown in Figure 3.*

	Algorithm	Gradient ($\nabla\tilde{\phi}$) (cycle/pixel)	$\Delta(\nabla\tilde{\phi})$ (%)	σ (cycle/pixel)
	Original	(0.1000, –0.1000)	(—,—)	0.149
(a)	LS-DCT	(0.0742, –0.0731)	(–25.8, –27.0)	0.179
(b)	RC	(0.0912, –0.0896)	(–8.7, –10.4)	0.168
(c)	RC + DC	(0.0956, –0.0951)	(–4.4, –4.9)	0.168

of DC will have an obvious effect on the unwrapping process. Hence, the accuracy of the unwrapped phase will be improved and the computation time will be reduced, as shown later. The unwrapped phase results obtained by the least-square method by using discrete cosine transform (LS-DCT) method [12], the RC method [2], and the proposed algorithm are shown in **Figs. 3(f) and 3(h)** with contour lines. To evaluate the characteristics of the phase unwrapping methods, we can count the number of contour lines in the unwrapped results and compare them with the number of stripes in the wrapped data, shown in **Fig. 3(b).** From the comparison, we can find that the number of lines in the unwrapped results is less than that in the wrapped phase data. The wrapped phase data has 20 lines, the unwrapped result of LS-DCT method has 14 lines, the unwrapped result of RC algorithm has 17 lines, and the proposed algorithm's result has 18 lines. The unwrapped result of the proposed algorithm has the nearest number of lines to wrapped data, which shows the highest accuracy. Moreover, the accuracy of the proposed algorithm can be emphasized, as shown in **Table 1**, which shows a quantitative comparison of the original and unwrapped phase map gradients. The gradients shown in the second column are obtained by fitting them to a planar function and the σ denotes the mean residual that is defined as a square root of a mean square residual from the fitted function. The σ of the original phase data is not equal to zero, because the original data contains noise with the given standard deviation. The error of gradients shown in the third column is estimated as the normalized difference between the unwrapped result and the original one, where the normalizing factor is the reciprocal of original one. From the table, it can be observed that the proposed algorithm, RC+DC, gives the smallest error in terms of the error of gradients. This is due to the consideration of adjoining pair definition in computation of the compensators in the proposed algorithm. This result confirms that the proposed method (RC+DC) reduces the phase errors that exist mainly in the original RC method. **Figure 4** shows a comparison of required computational time of LS-DCT and RC methods and the proposed RC+DC method for various image sizes; the horizontal axis N denotes one-dimensional area size in pixels. From the figure, the profile of the RC method and that of the proposed method show that the computation time is proportional to N^4. Furthermore, from Eq. (8), we can note that the time cost to compute the RC for all segments is proportional to the product of both the number of SPs and the number of the segments of path to be compensated. Since both are proportional to the area size ($\propto N^2$), the total evaluation time is proportional to N^4. In the proposed algorithm, if the cost to compute the DC is adequately smaller than that of RC, the total cost might be

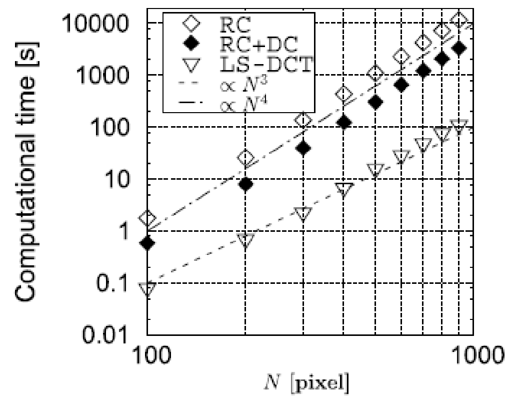

Figure 4*: Required computational time of each algorithm for various image sizes. The horizontal axis N denotes one-dimensional area size in pixels. RC shows the required time cost for RC method, RC+DC shows the required execution time for the proposed method, and LS-DCT shows the required time cost for LS-DCT method. The computational time is measured with a PC including an Intel Core 2 DUO central processing unit (CPU) with a 2:13GHz clock in the single CPU operation mode.*

similar to the case of the RC algorithm. Conversely, when the number of the times using DC computation is larger than that of RC in the proposed method, its execution time will be reduced compared to the RC algorithm case. As a result, by coupling RC and DC computations, the execution time of the proposed method is almost one third of the execution time of the original RC method. In contrast, the computational time of LS-DCT method increases with N^3. In this computation, we use a matrix form of 2D discrete Fourier transform. Through the use of matrix form, the computational time of 2D cosine transform needs only N^3 multiplications.

Experimental Results

The proposed algorithm has also been tested experimentally on a 2D wrapped phase map that resulted from the analysis of a real fringe pattern taken from the experiment carried out by using an interferometer. The purpose of this experiment is to measure the phase shift in candle flames. In this experiment, the exposure time cannot be set long enough because the flame is varying in time by convection flow around the flame itself. Therefore, the fringe pattern has low signal-to-noise ratio; hence, it contains some defects. The phase data has image size 256 pixels × 170 pixels and 2532 SPs (1267 positive SPs and 1265 negative SPs). The wrapped phase data and its corresponding SPs distribution map are shown in **Figs. 5(a)** and **5(b)**, respectively. Moreover, the unwrapped results, which have contour lines, obtained by RC method and the proposed algorithm are given in **Figs. 5(c)** and **5(d)**, respectively. By comparing the number of stripe lines in the wrapped phase data and the number of contour lines in the unwrapped results from the midpoint on the base line of each figure, it can be observed that the wrapped data has 10 lines, the unwrapped result of the RC algorithm has eight lines, and the proposed algorithm's result has nine lines. The unwrapped results in both methods are underestimated; however, the

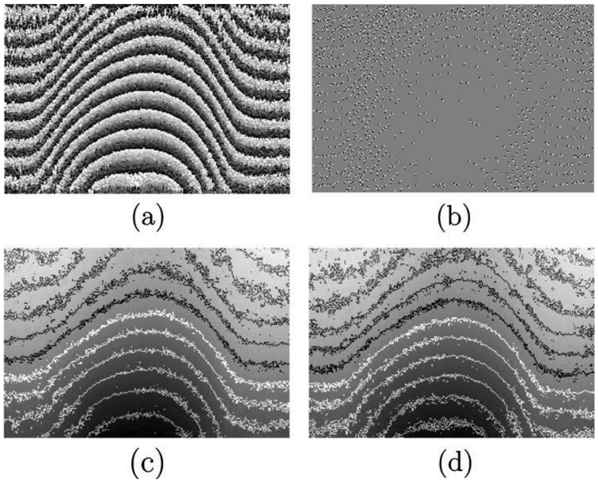

***Figure 5**: Unwrapped phase result of experimental data for candle flame: (a) the wrapped data, (b) SPs distribution map, (positive and negative SPs are represented by white and black dots, respectively); (c) the unwrapped result of RC algorithm, (d) the unwrapped result of RC+DC method.*

underestimation in the proposed algorithm is smaller than that in the RC method. This implies that the proposed algorithm succeeds to reduce the phase errors produced by the original RC method.

Conclusions

Several methods have been developed to solve phase unwrapping problems; nevertheless, providing satisfactory results leads to a time-consuming process. Phase unwrapping for noisy data by RC had higher accuracy than the other existing methods. However, it has a drawback of computational time requirement. To overcome this drawback, we propose a new method based on coupling the existing RC and the DC. The DC compensates the singularity of the pair of adjoining SPs connected by a branch cut with the length, which is shorter than 1 pixel. The compensator along the segment that crosses the branch cut is just 2π. For the SPs that are not members of adjoining pairs, RC is applied as a compensator. The proposed algorithm was tested on both computer-simulated and experimental noisy phase data. The results show that the proposed algorithm has a smaller computational time requirement compared to the original RC method, however, the execution time of the LS-DCT method is the least. Furthermore, the proposed method provides a more accurate unwrapped phase map than the past methods did.

References

1- S. Heshmat, S. Tomioka, and S. Nishiyama, “Reliable phase unwrapping algorithm based on rotational and direct compensators,” Appl. Opt. 50, 6225 – 6233 (2011).

2- S. Tomioka, S. Heshmat, N. Miyamoto, and S. Nishiyama, “Phase unwrapping for noisy phase maps using rotational compensator with virtual singular points,” Appl. Opt. 49, 4735–4745 (2010).

3- R. M. Goldstein, H. A. Zebker, and C. L. Werner, “Satellite radar interferometry: Two-dimensional phase unwrapping,” Radio Science 23, 713–720 (1988).

4- J.M. Huntley, “Noise-immune phase unwrapping algorithm,” Appl. Opt. 28, 3268–3270 (1989).

5- J. R. Buckland, J. M. Huntley, and S. R. E. Turner, “Unwrapping noisy phase maps by use of a minimum-cost-matching algorithm,” Appl. Opt. 34, 5100–5108 (1995).

6- R. Cusack, J. M. Huntley, and H. T. Goldrein, “Improved noise-immune phaseunwrapping algorithm,” Appl. Opt. 34, 781–789 (1995).

7- T. J. Flynn, “Two-dimensional phase unwrapping with minimum weighted discontinuity,” Opt. Soc. Am. A. 14, 2692 – 2701 (1997).

8- S. A. Karout, M. A. Gdeisat, D. R. Burton, and M. J. Lalor, “Two-dimensional phase unwrapping using a hybrid genetic algorithm,” Appl. Opt. 46, 730–743 (2007).

9- D. L. Fried, “Least-square fitting a wave-front distortion estimate to an array of phase difference measurements,” Opt. Soc. Am. 67, 370–375 (1977).

10- H. Takajo and T. Takahashi, “Least-squares phase estimation from the phase difference,” Opt. Soc. Am. A 5, 416–425 (1988).

11- D. C. Ghiglia and L. A. Romero, “Direct phase estimation from phase differences using fast elliptic partial differential equation solvers,” Opt. Lett. 14, 1107–1109 (1989).

12- D. C. Ghiglia and L. A. Romero, “Robust two-dimensional weighted and unweighted phase unwrapping that uses fast transforms and iterative methods,” Opt. Soc. Am. A 11, 107–117 (1994).

13- R. Yamaki and A. Hirose, “Singularity-spreading phase unwrapping,” IEEE Trans. Geoscience and Remote Sensing 45, 3240–3251 (2007).